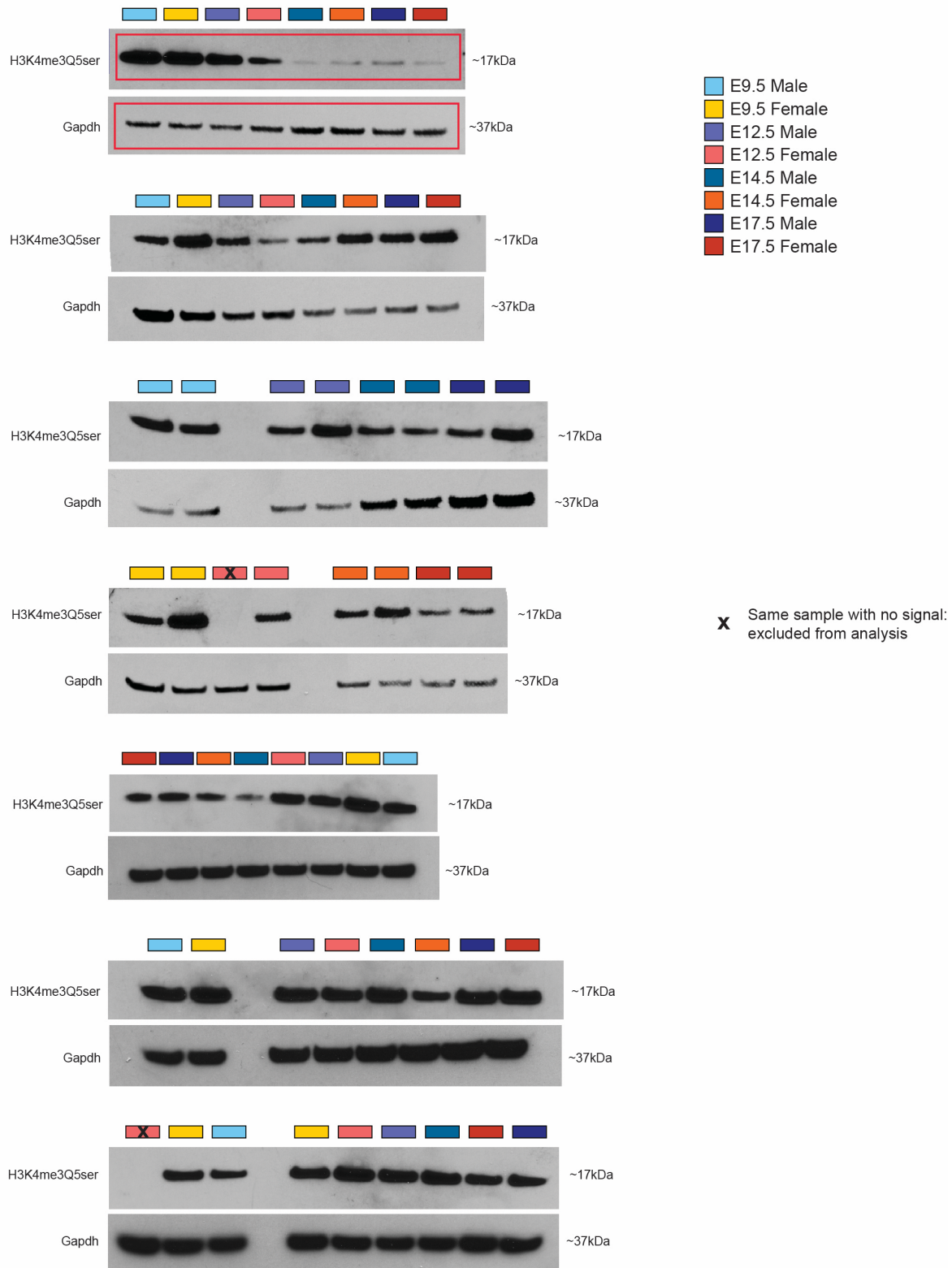


## 652 Supplementary Figure Captions

### Supplementary Figure 1



653

654 **Supplementary Figure 1. Western blots used for the quantification of the placental**

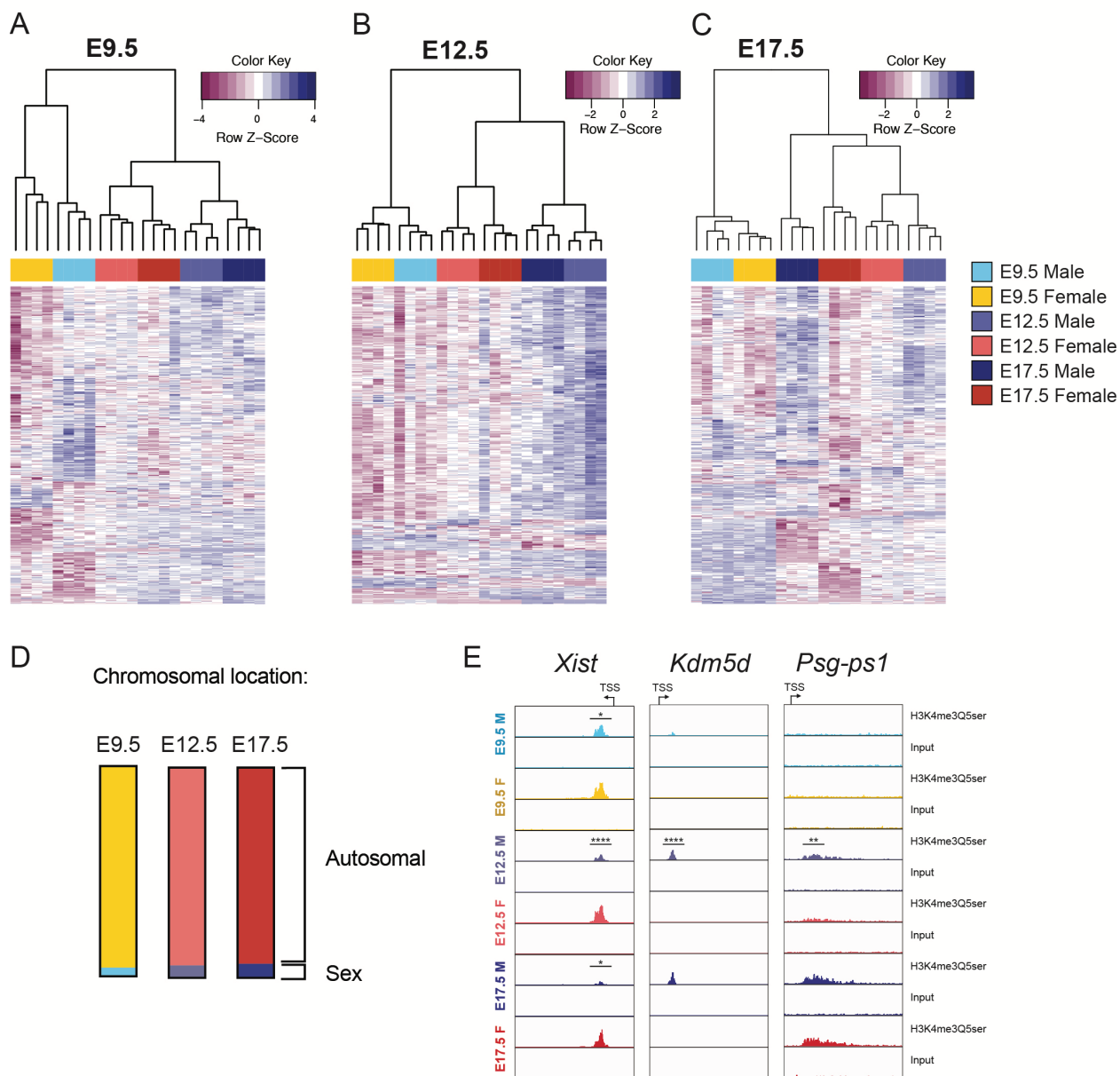
655 **H3K4me3Q5ser signal in Figure 1C**

656 Red rectangles indicate the representative blots displayed in the main figure. One sample (run two

657 times) was excluded due to lack of H3K4me3Q5ser signal (indicated by X).

658

## Supplementary Figure 2



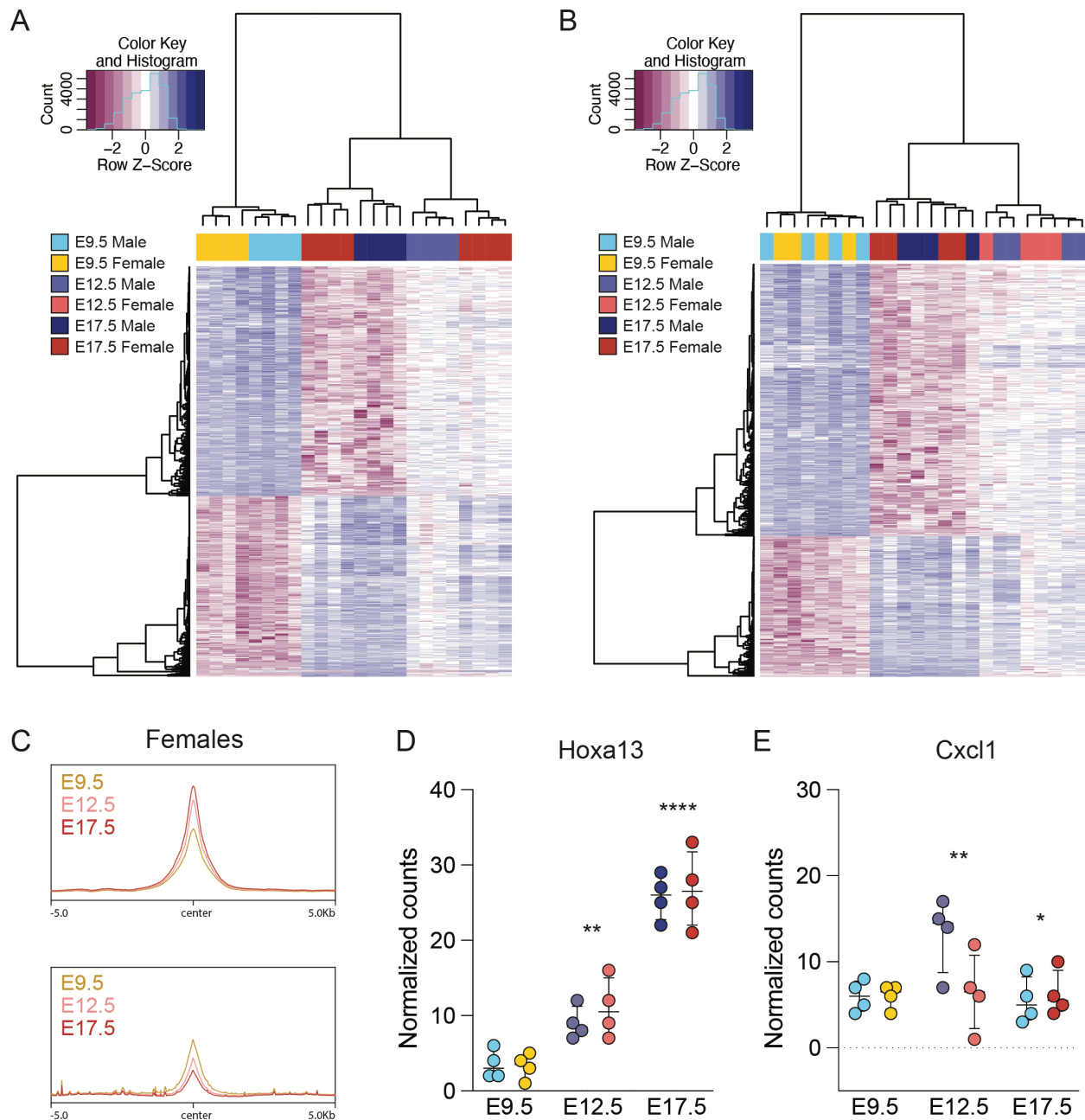
659

### 660 **Supplementary Figure 2. Sex differences in placental H3K4me3Q5ser**

661 (A-C) Heatmaps of top 500 differential peaks from Diffbind analysis ( $p < 0.05$ ) based on fold  
 662 change comparing male vs. female placental tissues within age at (A) E9.5, (B) E12.5, and (C)  
 663 E17.5 with hierarchical clustering (N=4 samples/sex/age). (D) Chromosomal location of all  
 664 significant ( $p < 0.05$ ) sex different peaks per age, where ~95% of peaks occurred on autosomal

665 chromosomes and 4-6% of peaks occurred on the X or Y chromosomes. **(E)** Representative  
666 genome browser tracks of sex different H3K4me3Q5ser peaks (vs respective DNA input on the X  
667 chromosome (*Xist*:  $p < 0.05$  relative to male at E9.5 and E17.5,  $p < 0.0001$  relative to male at  
668 E12.5), Y chromosome (*Kdm5d*:  $p < 0.0001$  relative to male at E12.5), and on chromosome 7 (*Psg-*  
669 *ps1*:  $p < 0.01$  relative to male at E12.5). Each track represents merged signal for 4 samples.  
670  
671

### Supplementary Figure 3



672  
673

674 **Supplementary Figure 3. Differential H3K4me3Q5ser enrichment in male and female**  
675 **placenta**

676

677 **(A-B)** Heatmaps of top 1000 differential peaks from Diffbind analysis ( $p < 0.05$ ) based on fold

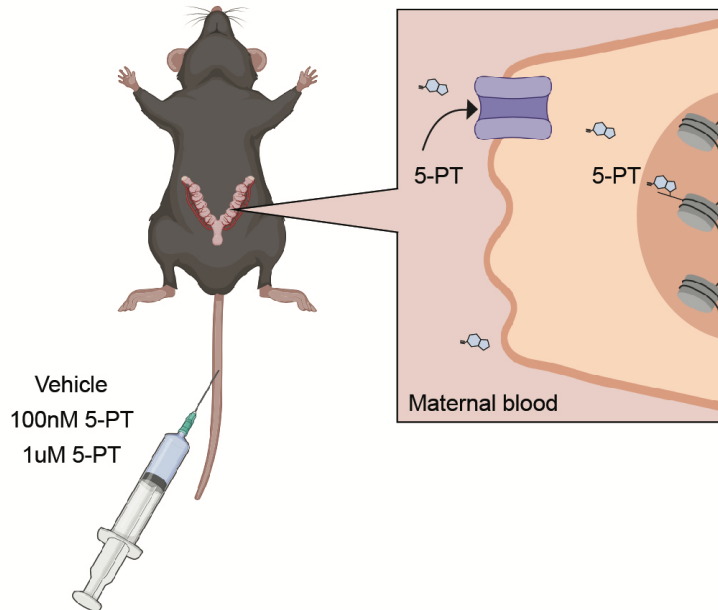
678 change comparing E9.5 vs E17.5 in male **(A)** and female **(B)** placental tissues with hierarchical

679 clustering, showing developmental changes are largely conserved across sexes (N=4

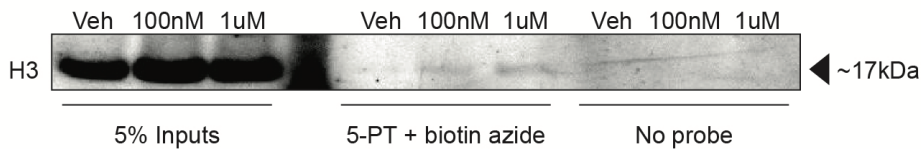
680 samples/sex/age). **(C)** Profiles of differential peaks from E9.5 vs E17.5 comparisons, separated by  
681 directionality and centered on genomic regions in females. **(D)** *Hoxa13* gene expression increases  
682 across development, corresponding with H3K4me3Q5ser increases (two-way ANOVA, effect of  
683 age:  $F(2,18) = 1108$ ,  $p < 0.0001$ ; Tukey's post-hoc, E9.5 vs E12.5:  $**p = 0.0016$ ; E12.5 vs E17.5:  
684  $****p < 0.0001$ ). **(E)** *Cxcl1* gene expression decreases from E12.5 to E17.5, similarly to  
685 H3K4me3Q5ser decreases at the same time points (two-way ANOVA, effect of age:  $F(2,18) =$   
686  $4.244$ ,  $p = 0.0309$ ; Tukey's post-hoc; E12.5 vs E17.5:  $*p = 0.049$ ).  $N = 4$ /sex/age. Data are median  
687  $\pm$  interquartile range.  
688

## Supplementary Figure 4

A



B



689

690 **Supplementary Figure 4. Detection of circulating propargylated 5-HT (5-PT) on placental**  
691 **histone H3**

692

693 (A) Schematics of experimental design and expected results. The alkyne-functionalized 5-HT

694 analogue, 5-PT, was injected into pregnant E12.5 mice at 100nM or 1µM (vs. vehicle).

695 Transporter-mediated mechanisms within the apical membrane of the placenta facing maternal

696 circulation would directly take up 5-PT into cells, increasing 5-PT addition to histone H3 as proxy

697 for how H3 seronylation might be regulated. One hour post-injection, placental tissues were

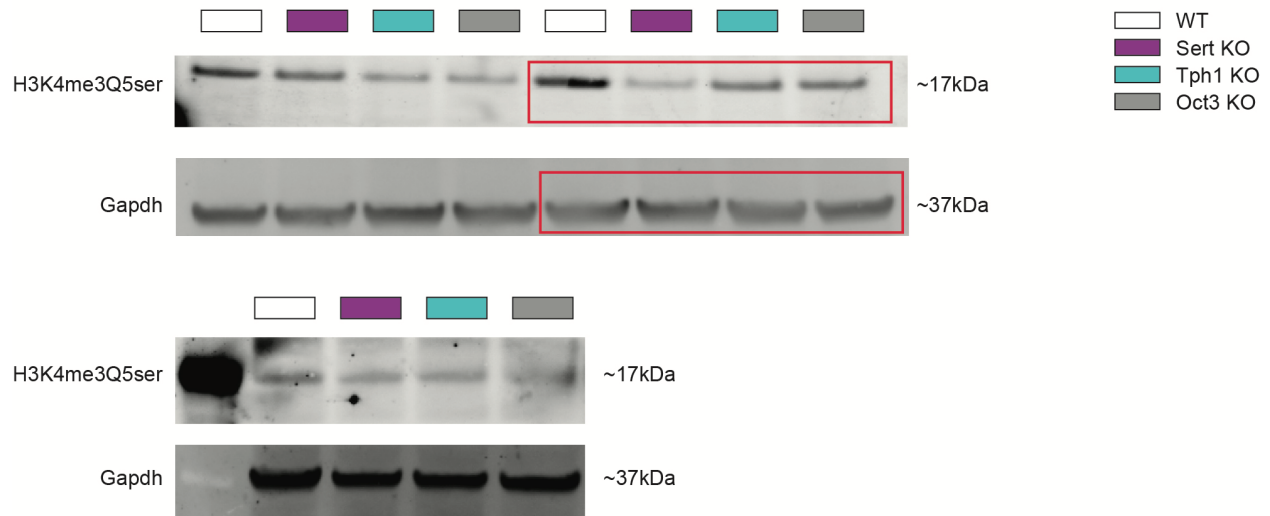
698 collected and subjected to copper-click chemistry using biotin azide (vs. no probe). 5-PT-ylated

699 proteins were immunoprecipitated with streptavidin beads, followed by western blotting for H3.

700 **(B)** Western blot showing H3 is enriched in 5-PT-treated samples in dose-dependent manner  
701 (compared to vehicle) only in click reaction conditions.  
702



## Supplementary Figure 5



703

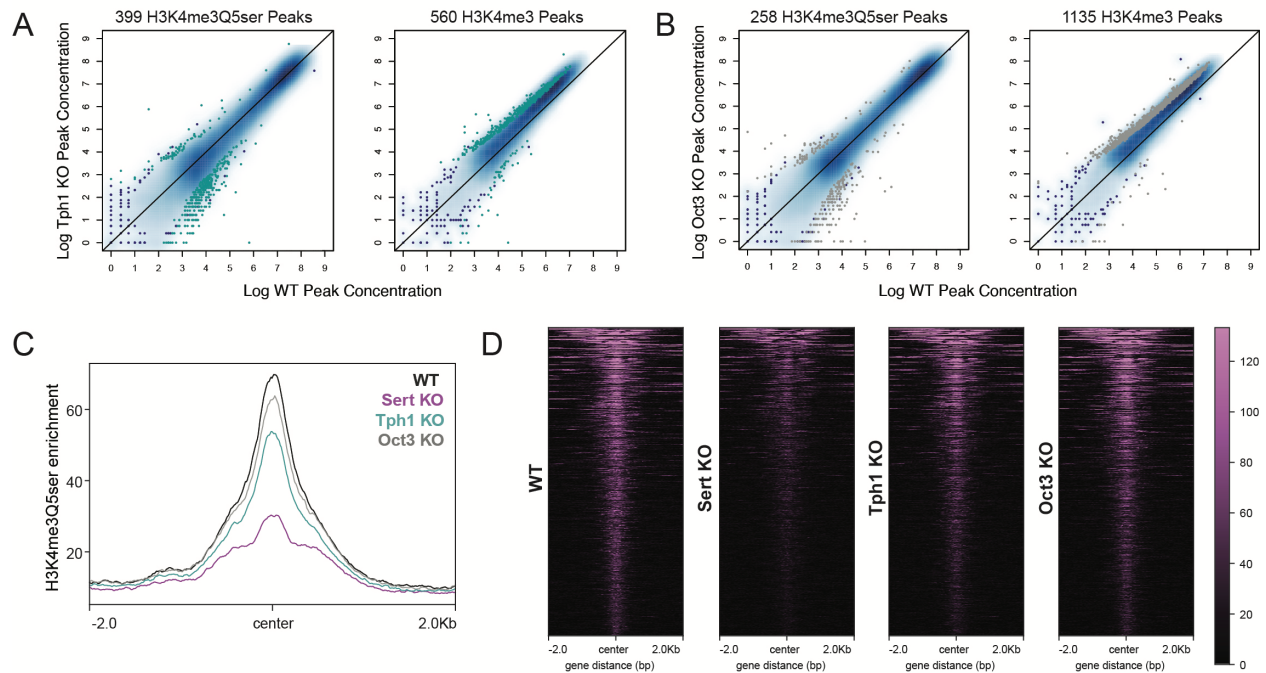
704 **Supplementary Figure 5. Western blots used for the quantification in Figure 2F.** Western

705 blots of placental tissues at E12.5, showing H3K4me3Q5ser in WT, Sert KO, Tph1 KO and Oct3

706 KO tissues. Red rectangles indicate the representative blots displayed in the main figure.

707

## Supplementary Figure 6



708

### 709 **Supplementary Figure 6. Histone seronylation reductions are most affected by deletion of** 710 **SERT**

711

712 (A-B) Scatterplots of differential H3K4me3Q5ser and H3K4me3 peaks in (A) Tph1 KO and (B)

713 Oct3 KO E12.5 placentas relative to WT ( $p < 0.05$ ). (C) Profiles and (D) heatmaps of all

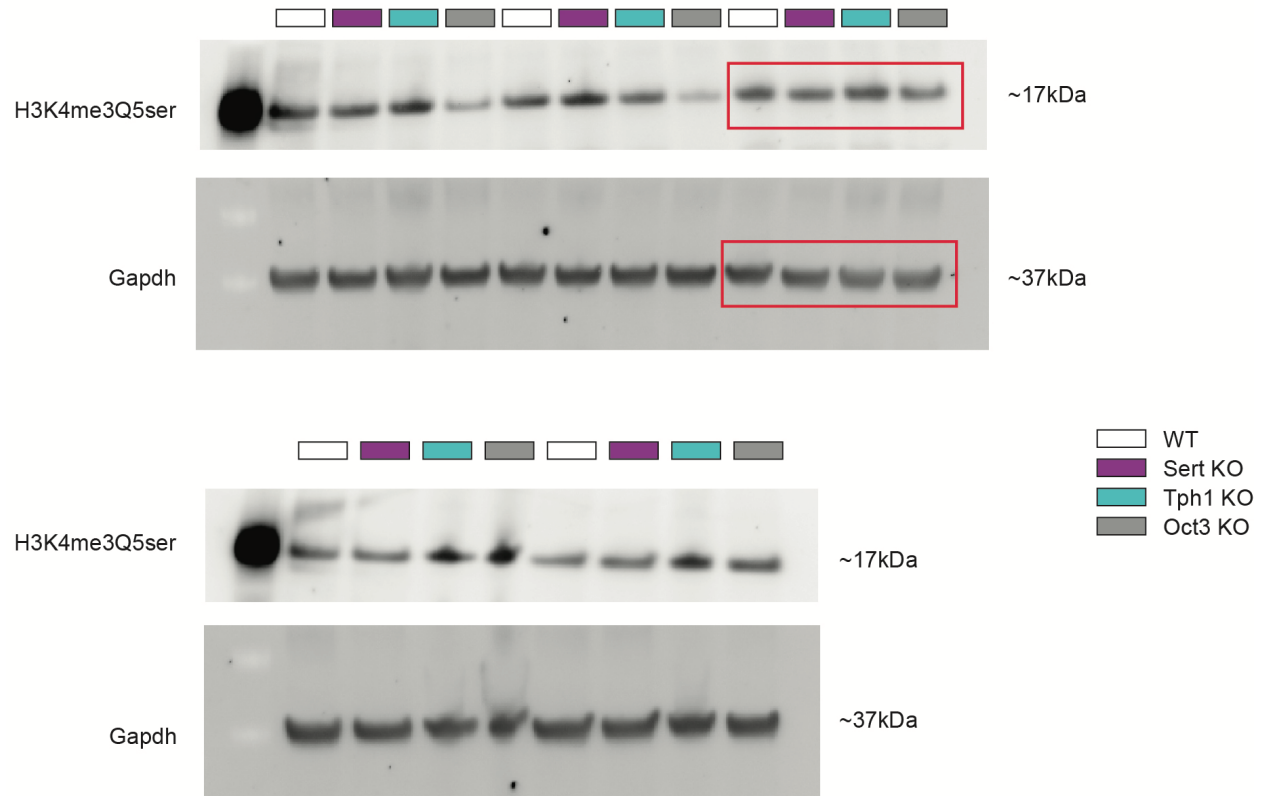
714 downregulated differential H3K4me3Q5ser loci comparing WT vs Sert KO placental tissues ( $p <$

715 0.05), showing Sert KO has the greatest impact on histone seronylation peak reductions

716 compared to Tph1 KO and Oct3 KO, consistent with reductions in 5-HT levels.

717

## Supplementary Figure 7



718

719 **Supplementary Figure 7. Western blots used for the quantification of H3K4me3Q5ser in**

720 **E12.5 brain tissues of WT, Tph1 KO, Sert KO, and Oct3 KO in Figure 4D. Red rectangles**

721 **indicate the representative blots displayed in the main figure.**

722

## 723 **Supplementary Table Captions**

724 Excel file including Supplementary Tables 1-28, which contain analyses of ChIP-seq and RNA-  
725 seq from placental and brain tissues.

726

727 **Supplementary Table 1:** Developmental placenta H3K4me3Q5ser ChIP-seq, DiffBind results  
728 (E9.5 male vs E17.5 male): Fig. 1E-J, Supplementary Fig. 3A

729

730 **Supplementary Table 2:** Developmental placenta H3K4me3Q5ser ChIP-seq, DiffBind results  
731 (E9.5 female vs E17.5 female): Fig. 1E, H, I, Supplementary Fig. 3B-C

732

733 **Supplementary Table 3:** Developmental placenta H3K4me3Q5ser ChIP-seq, DiffBind results  
734 (E9.5 male vs E9.5 female): Fig. 1E, Supplementary Fig. 2A

735

736 **Supplementary Table 4:** Developmental placenta H3K4me3Q5ser ChIP-seq, DiffBind results  
737 (E12.5 male vs E12.5 female): Fig. 1E, Supplementary Fig. 2B

738

739 **Supplementary Table 5:** Developmental placenta H3K4me3Q5ser ChIP-seq, DiffBind results  
740 (E17.5 male vs E17.5 female): Fig. 1E, Supplementary Fig. 2C

741

742 **Supplementary Table 6:** Developmental placenta bulk RNA-seq, normalized counts table

743

744 **Supplementary Table 7:** Developmental placenta bulk RNA-seq, DESeq2 results (E9.5 male vs  
745 E17.5 male): Fig. 1I, Supplementary Fig. 3D-E

746

747 **Supplementary Table 8:** Developmental placenta bulk RNA-seq, DESeq2 results (E9.5 female  
748 vs E17.5 female): Fig. 1I, Supplementary Fig. 3D-E

749

750 **Supplementary Table 9:** Developmental placenta functional annotation analysis, Gene Ontology  
751 Biological Processes (E9.5 male vs E17.5 male): Fig. 1K

752

753 **Supplementary Table 10:** Developmental placenta functional annotation analysis, Reactome  
754 (E9.5 female vs E17.5 female): Fig. 1K

755

756 **Supplementary Table 11:** Transgenic placenta H3K4me3Q5ser ChIP-seq, DiffBind results (WT  
757 vs Sert KO): Fig. 3A-C, Supplementary Fig. 7C-D

758

759 **Supplementary Table 12:** Transgenic placenta H3K4me3 ChIP-seq, DiffBind results (WT vs Sert  
760 KO): Fig. 3A, 3C

761

762 **Supplementary Table 13:** Transgenic placenta H3K4me3Q5ser ChIP-seq, DiffBind results (WT  
763 vs Tph1 KO): Fig. 3A, 3C, Supplementary Fig. 7A

764

765 **Supplementary Table 14:** Transgenic placenta H3K4me3 ChIP-seq, DiffBind results (WT vs  
766 Tph1 KO): Fig. 3A, 3C, Supplementary Fig. 7A

767 **Supplementary Table 15:** Transgenic placenta H3K4me3Q5ser ChIP-seq, DiffBind results (WT  
768 vs Oct3 KO): Fig. 3A, 3C, Supplementary Fig. 7B  
769

770 **Supplementary Table 16:** Transgenic placenta H3K4me3 ChIP-seq, DiffBind results (WT vs  
771 Oct3 KO): Fig. 3A, 3C, Supplementary Fig. 7B  
772

773 **Supplementary Table 17:** Transgenic placenta functional annotation analysis, Gene Ontology  
774 Biological Processes (WT vs Sert KO): Fig. 3G  
775

776 **Supplementary Table 18:** Transgenic placenta functional annotation analysis, Gene Ontology  
777 Biological Processes (WT vs Tph1 KO): Fig. 3G  
778

779 **Supplementary Table 19:** Transgenic placenta functional annotation analysis, Gene Ontology  
780 Biological Processes (WT vs Oct3 KO): Fig. 3G  
781

782 **Supplementary Table 20:** Transgenic brain bulk RNA-seq, normalized counts table  
783

784 **Supplementary Table 21:** Transgenic brain bulk RNA-seq, DESeq2 results (WT vs Sert KO):  
785 Fig. 4E-F  
786

787 **Supplementary Table 22:** Transgenic brain bulk RNA-seq, DESeq2 results (WT vs Tph1 KO):  
788 Fig. 4E-F  
789

790 **Supplementary Table 23:** Transgenic brain bulk RNA-seq, DESeq2 results (WT vs Oct3 KO):  
791 Fig. 4E-F  
792

793 **Supplementary Table 24:** Transgenic brain bulk RNA-seq functional annotation analysis, Gene  
794 Ontology Biological Processes (WT vs Sert KO): Fig. 4G  
795

796 **Supplementary Table 25:** Transgenic brain bulk RNA-seq functional annotation analysis,  
797 Reactome (WT vs Sert KO): Fig. 4G  
798

799 **Supplementary Table 26:** Transgenic brain bulk RNA-seq functional annotation analysis, Gene  
800 Ontology Biological Processes (WT vs Oct3 KO): Fig. 4G  
801

802 **Supplementary Table 27:** Transgenic brain bulk RNA-seq functional annotation analysis,  
803 Reactome (WT vs Oct3 KO): Fig. 4G  
804

805 **Supplementary Table 28:** Transgenic brain bulk RNA-seq functional annotation analysis,  
806 Reactome (WT vs Tph1 KO): Fig. 4G  
807  
808